A microbial fuel cell in contaminated ground delineated by electrical self-potential and normalized induced polarization data

Doherty, R., Kulessa, B., Ferguson, A., Larkin, M., Kulakov, L., & Kalin, B. (2010). A microbial fuel cell in contaminated ground delineated by electrical self-potential and normalized induced polarization data. Journal of Geophysical Research: Biogeosciences, 115(G3), [G00G08]. DOI: 10.1029/2009JG001131

Published in:
Journal of Geophysical Research: Biogeosciences

Document Version:
Peer reviewed version

Queen's University Belfast - Research Portal:
Link to publication record in Queen's University Belfast Research Portal

A microbial fuel cell in contaminated ground delineated by electrical self-potential and normalized induced polarization data

R. Doherty,[1] B. Kulessa,[2,3] A. S. Ferguson,[3,4] M. J. Larkin,[5] L. A. Kulakov,[5] and R. M. Kalin[6]

Received 25 August 2009; revised 13 February 2010; accepted 4 March 2010; published XX Month 2010.

[1] There is a growing interest in the use of geophysical methods to aid investigation and monitoring of complex biogeochemical environments, for example delineation of contaminants and microbial activity related to land contamination. We combined geophysical monitoring with chemical and microbiological analysis to create a conceptual biogeochemical model of processes around a contaminant plume within a manufactured gas plant site. Self-potential, induced polarization and electrical resistivity techniques were used to monitor the plume. We propose that an exceptionally strong (>800 mV peak to peak) dipolar SP anomaly represents a microbial fuel cell operating in the subsurface. The electromagnetic and electrical geophysical data delineated a shallow aerobic perched water body containing conductive gasworks waste which acts as the abiotic cathode of microbial fuel cell. This is separated from the plume below by a thin clay layer across the site. Microbiological evidence suggests that degradation of organic contaminants in the plume is dominated by the presence of ammonium and its subsequent degradation. We propose that the degradation of contaminants by microbial communities at the edge of the plume provides a source of electrons and acts as the anode of the fuel cell. We hypothesize that ions and electrons are transferred through the clay layer that was punctured during the trial pitting phase of the investigation. This is inferred to act as an electronic conductor connecting the biologically mediated anode to the abiotic cathode. Integrated electrical geophysical techniques appear well suited to act as rapid, low cost sustainable tools to monitor biodegradation.

Citation: Doherty, R., B. Kulessa, A. S. Ferguson, M. J. Larkin, L. A. Kulakov, and R. M. Kalin (2010), A microbial fuel cell in contaminated ground delineated by electrical self-potential and normalized induced polarization data, *J. Geophys. Res.*, *115*, XXXXXX, doi:10.1029/2009JG001131.

1. Introduction

[2] The use of sustainable remediation methods, such as e.g., permeable reactive barriers, at complex contaminated sites requires an insightful and multidisciplinary approach [*Kalin*, 2004; *Gibert et al.*, 2007]. The regulatory level of detail required to monitor permeable reactive barriers, coupled with the elevated costs of in situ and laboratory analyses can quickly render this environmentally friendly approach to brownfield risk management and remediation unsustainable. The need for novel, low cost, low impact and sustainable remediation methods and monitoring tools are critical if brownfield redevelopment issues are to be addressed economically [*Spira*, 2006]. This paper applies electrical geophysical methods such as self-potential, induced polarization and resistivity to a site with a contaminant plume that is managed by a permeable reactive barrier. Electrical geophysical methods have been applied as an investigation and monitoring method to determine a variety of environmental conditions. The self-potential method measures the electrical potential that arises from natural current flow in the subsurface, which is often due to complex and non-unique mechanisms. A principal source mechanism is subsurface fluid flow as an electrical charge separation occurring between the solid matrix and the pore

[1]Environmental Engineering Research Centre, School of Planning Architecture and Civil Engineering, Queen's University of Belfast, Belfast, UK.
[2]School of the Environment and Society, Swansea University, Swansea, UK.
[3]Formerly at Environmental Engineering Research Centre, School of Planning Architecture and Civil Engineering, Queen's University of Belfast, Belfast, UK.
[4]Department of Civil Engineering and Engineering Mechanics, Columbia University, New York, New York, USA.
[5]QUESTOR Centre and School of Biological Sciences, Queen's University of Belfast, Belfast, UK.
[6]David Livingstone Centre for Sustainability, Department of Civil Engineering, Strathclyde University, Glasgow, UK.

0148-0227/10/2009JG001131

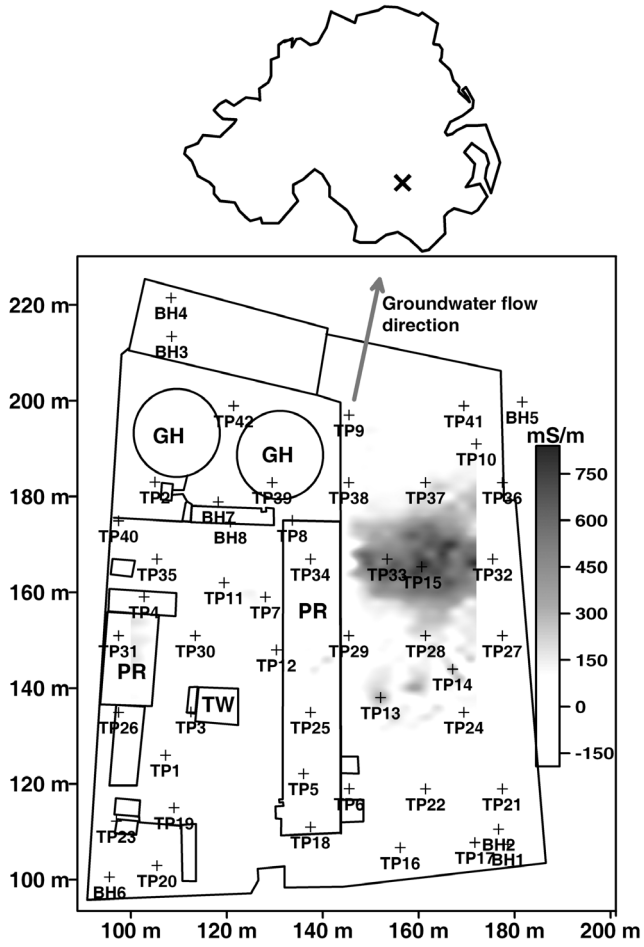

Figure 1. Location (cross) and site plan of the former manufactured gas plant at Portadown, Northern Ireland, with sample locations on a local grid using an arbitrary datum. Labels of foundations of demolished infrastructure prior to remediation are as follows: GH = gas-holding tanks, TW = Tar Well, PR = Purifiers, TP = Trial Pit, BH = Borehole. The reconnaissance EM31 apparent conductivity data (in mS/m) are characterized by a strongly conductive anomaly in the eastern sector of the site.

fluid (electrical streaming potential). This has identified piezometric surfaces utilizing the electrokinetic properties of water rock interaction [*Fournier*, 1989; *Revil et al.*, 2003; *Linde et al.*, 2007]. Another principal self-potential mechanism is due to electrochemical processes resulting in the diffusion of ions. The self-potential electrochemical potentials arising from chemical gradients has been used to monitor groundwater tracer tests [*Sandberg et al.*, 2002] and to define mixing of glacial meltwaters [*Kulessa et al.*, 2003]. Redox driven electrochemical gradients have produced self-potential signals associated with ore deposits [*Sato and Mooney*, 1960; *Bigalke and Grabner*, 1997] which coined the term 'geobattery' and more recently with contaminant plumes [*Naudet et al.*, 2004, *Arora et al.*, 2007; *Minsley et al.*, 2007]. Laboratory work has helped to define the relationship between self-potential and redox potential [*Maineult et al.*, 2006; *Castermant et al.*, 2008; *Revil et al.*, 2009] where the self-potential should be constrained by the range of Eh and should require the presence of an electronic conductor. In addition to these traditionally recognized self-potential sources, microbially mediated coupled ion-electron flows have recently emerged as a subset of the electrochemical mechanism for natural subsurface current flow [*Revil et al.*, 2010]. Microbially mediated redox environments may produce electronic conductors through the bioprecipitation of minerals allowing bio-geobatteries to occur [*Naudet and Revil.*, 2005]. The electrical resistivity and induced polarization methods respectively exploit the resistance of the subsurface to the flow of an injected current, and the ability of the subsurface to store electrical charge [*Reynolds*, 1997; *Sharma*, 1997]. Laboratory experiments using induced polarization have identified biomineralization [*Slater et al.*, 2007; *Personna et al.*, 2008] microbial presence [*Ntarlagiannis et al.*, 2005; *Davis et al.*, 2006] and artificial biofilms [*Ntarlagiannis and Ferguson*, 2009]. Field applications of induced polarization with respect to contamination issues have focused on monitoring of remediation performance [*Slater and Binley*, 2006; *Williams et al.*, 2009]. This work compiles investigation and monitoring using electrical geophysical methods at a former manufactured gas plant site with a PRB to create a conceptual biogeochemical model of processes associated with a contaminant plume. We present a field-scale case study that considers self-potential, induced polarization and electrical resistivity applied to characterize a complex contaminant plume. More specifically, the electrical geophysical data are used to update the biogeochemical model of the complex contaminant plume, and propose a microbial fuel cell operating in the subsurface that is an indicator of the biodegradation process.

2. Site Description

[3] The site is a former manufactured gas plant at Portadown, Northern Ireland; it occupies an area of approximately 1 ha and had been operational for over one hundred years. The west of the site contained the foundations of demolished structures such as the gas-holding tanks and tar well (Figure 1). The eastern sector of the site contained dumped gasworks waste in the north with undisturbed alluvial sediments in the south. During 1999, a series of multi disciplinary investigation work was undertaken to assess the level of subsurface contamination [*Ferguson et al.*, 2003]. A risk management strategy (a permeable reactive barrier) was implemented during 2001 and monitoring at the site has continued to the present. A time line of investigation, risk management and monitoring at the site is outlined in Table 1.

3. Methodology

3.1. Reconnaissance EM Geophysical Surveys

[4] Reconnaissance electromagnetic geophysical surveys on a 10 m × 10 m grid, using three different GEONICS EM instruments, provided direction for the intrusive site investigation. As described in most textbooks of environmental geophysics [e.g., *Reynolds*, 1997; *Sharma*, 1997], electromagnetic geophysical methods consider the generation of a primary electromagnetic field at the ground surface using one coil in the survey instrument. The electromagnetic response of the subsurface to that primary field is measured with a

t1.1 **Table 1.** Timeline of Investigation, Remediation, and Monitoring
t1.2 at the Manufactured Gas Plant Site, Portadown, Northern Ireland

t1.3 Date	Event
t1.4 1880s–1980s	Operational life of the Manufactured Gas Plant (Gasworks)
t1.5 March 1999	First geophysical survey using EM31, EM38, and EM61
t1.6 May–July 1999	Intrusive site investigation 43 trial pits and 8 boreholes
t1.7 June 2001–October 2002	Installation of cement bentonite slurry wall and Permeable reactive barrier treatment zone
t1.8 October 2002 - present	Monitoring of permeable reactive barrier treatment zone
t1.9 March 2005	Geophysics survey of contaminant plume using self-potential, induced polarization and resistivity

second instrument coil. Comparison of the signal characteristics of this secondary electromagnetic field with the primary field allows conductive materials in the subsurface to be detected and laterally delineated. The underlying physical principle focuses on the secondary electromagnetic field being generated by eddy currents induced by the primary field in conductive subsurface materials. Thus, the more conductive the subsurface material, the stronger the eddy currents and the stronger the secondary electromagnetic field. The depth of penetration and spatial resolution depends on the electromagnetic instrument utilized. In the present case GEONICS EM-61, EM-38 and EM-31 were used, designed respectively as a metal detector, a soil salinity probe and a bulk ground-conductivity sensor.

3.2. Intrusive Site Investigation and Chemical and Microbial Sampling and Analyses

[5] The intrusive site investigation was carried out in two phases. The first phase involved forty three trial pits to a maximum depth of 5m with soil and groundwater samples recovered at regular intervals for contaminant chemistry and microbial analysis. The contaminant chemistry analysis for soil and water samples from trial pit was carried out at an accredited laboratory (Geochem, Chester, UK). The analysis suite included inorganic contaminants (ammonium, cyanide, sulphur, and sulphate), metals (As, Cr, Cu, Ni, Pb, Se, Zn, and Hg) and organic contaminants (solvent extractable matter, mineral oil, non-volatile aromatics, and resins). Based on the trial pit contaminant chemistry results, eight boreholes were drilled and emplaced with multi level piezometers to be used in conjunction with the risk management strategy adopted at the site. Microbial analysis from the trial pit samples included enumeration of microorganisms, cloning 16S rRNA genes and sequencing. Total viable counts of aerobic heterotrophic bacteria were enumerated and bacteria were isolated using R2A agar plates (OXOID Ltd.) We also extracted DNA for Polymerase chain reaction amplification. DNA extraction used the FastDNA SPIN Kit for Soil (BIO 101) and followed the manufacturer's protocol. DNA samples were chronologically logged and stored for future reference. After DNA extraction from soil the 16S rDNA genes were amplified by PCR (primers 8F and 518R from [*Leu et al.*, 1998]). The ~500 kb DNA fragments were purified, cloned into pUC129, and transferred into *E. coli* DH5a [*Sambrook et al.*, 1989]. The clones (over 100) were then analyzed by restriction analysis using three restriction enzymes (*Alu*I, *Rsa*I, and *Hpa*II) to eliminate identical clones. All the clones showing a different restriction pattern were sequenced in-house using the Beckman CEQ2000 automated sequencer. For the purpose of the initial phylogenetic identification, obtained sequences were compared to GenBank entries using BLAST engine (http://blast.ncbi.nlm.nih.gov/Blast.cgi).

3.3. Conceptual Contaminant Transport Model

[6] The data from the site investigation were used to create a conceptual and numerical groundwater-flow model of the site. The model was calibrated and verified during a dewatering phase to remove the gas holding tank foundations (Figure 1) prior to cement bentonite slurry wall construction [*Doherty et al.*, 2003]. A simple contaminant transport model was constructed using the tar well on the site as a continuous source of 500 mg/L of phenanthrene. This well had been recorded at the site from its inception, and was inferred to be the main source of groundwater contamination based on the synthesized post-investigation model of the site. Phenanthrene was chosen as representative organic compound migrating in groundwater owing to its recalcitrant nature in terms of mobility and solubility. Other potential sources of contamination, such as from buildings or dumped gasworks waste, were not considered because the duration of a continuous contaminant source could not be established. The contaminant model was run for a period of one hundred years to mimic the transport of the more recalcitrant polycyclic aromatic hydrocarbons over the history of the site.

3.4. Electrical Geophysical Surveys in Support of Remediation Monitoring

[7] The longer-term risk management strategy of the soil and groundwater contamination focused on the installation of a permeable reactive barrier at the down flow boundary of the site, along with a cement bentonite slurry wall for groundwater management through the permeable reactive barrier. During March 2005 as part of the remediation monitoring process, self-potential data were collected at a total of 110 measurement stations on a 5m × 5m grid, covering an area of 45 × 50 m (2250m^2). These surveys were complemented by ten parallel induced polarization and electrical resistivity profiles that were co-located with the self-potential grid locations in an East-to-West direction. The electrical geophysical survey area focused on the central portion of the site covering pristine natural ground, known contamination and anomalies identified by the reconnaissance electromagnetic geophysical surveys.

[8] In the absence of significant thermally generated self-potentials, we expect our raw self-potential data to be an integrated signature of streaming, electrochemical and biologically mediated electrical potentials. We used off-the-shelf non-polarizing Pb-PbCl electrodes [*Petiau*, 2000] for our self-potential surveys, together with a METRA HIT 22S high-impedance multimeter and rugged single-core wire. To ensure good and laterally uniform electrode contact, all self-potential monitoring locations consisted of a 0.30 m deep hole filled with a viscous bentonite slurry. The reference electrode was located in a pristine area of the site, and we followed standard practice in collecting and drift-correcting self-potential data with the roving electrode relative to this refer-

ence electrode [*Reynolds*, 1997; *Sharma*, 1997]. More specifically, all survey lines were connected with each other using numerous tie-in points, forming loops [*Naudet et al.*, 2004]. Loop-closure errors were re-distributed over the measurement stations in any particular loop, and were generally minute compared to the self-potential anomalies (several 100 millivolts) interpreted here. We adopted the methodology pioneered by *Naudet et al.* [2004] in isolating the streaming potential contribution to, and subtracting this contribution from, the total measured self-potential map.

[9] Resistivity and induced polarization data are usually collected using dedicated instrumentation that switches automatically between series of quadripoles, where respectively two stainless-steel electrodes are used to inject the current at the ground surface and measure the ground's voltage response. Stainless-steel electrodes were readily available in the required quantity and expected to perform acceptably well [*LaBrecque and Daily*, 2008]; although we recognize that other electrode materials may have been preferable. Here we used an IRIS *Syscal R1Plus Switch 36* imaging system (www.iris-instruments.com) for data collection, with an array of 36 electrodes spaced 2 m apart, in the *Wenner* configuration, along the ten profiles spanned by the East-West nodes of the self-potential grid. The induced polarization and resistivity data were subsequently inverted tomographically in 2-D using the Res2Dinv software using the default inversion settings [*Loke and Barker*, 1996] inverting resistivity and IP concurrently, inferring the spatial distribution of resistivity and chargeability. Inversions typically converged within five iterations with a root mean square error of less than five percent. Chargeability expresses the magnitude of the induced polarization effect in the time domain, as manifested in a residual voltage after termination of current injection [*Slater and Lesmes*, 2002]. The induced polarization and resistivity data were interpolated in 3-D by the inverse distance method using the commercially available Voxler software (www.goldensoftware.com). The resistivity of in situ near surface materials is principally a function of the electrical properties of the fluids in the pore space. Chargeability is a function of both the pore fluid electrical properties and those of the interface between the solid matrix and the fluid-bearing pore space within it in the absence of continuous electronic conductors. [*Slater and Lesmes*, 2002]. The important implication is that normalization of chargeability by resistivity can eliminate pore fluid effects and therefore emphasize the electrical properties of the solid matrix [*Slater and Lesmes*, 2002].

4. Results

4.1. Reconnaissance Electromagnetic and Water and Soil Quality Surveys

[10] The EM-31 and EM-38 bulk ground conductivity data, obtained prior to the intrusive investigation, identified a conductive anomaly of up to ~ 800 ms m^{-1} (Figure 1). Three trial pits (TPs 15, 32, 33; Figure 1) were excavated in this area to a maximum depth of 2.2 m. All three trial pits produced dark ashy metallic clinker and miscellaneous gravel sized particles with occasional fused iron to a depth of 1.7–1.8m where natural ground in the form of a clay aquiclude was encountered. This clay layer was found throughout the site and varied in thickness from 0.5m to 2.5m. The lithologies encountered were alluvial clays overlying interbedded sands and silts which lay on stiff glacial clays. Subsequent analysis of soils and perched waters from the fill material in TPs 15, 32 and 33 confirmed that contamination was not of concern in this area. Field measurements of the perched groundwater, at temporary installations using a multimeter and flow cell, revealed fluid electrical conductivities of 1210–1460 μS/cm conductivity, dissolved oxygen levels of 0.11–1.01 ppm, redox potentials (Eh) of 67–97mV, and pHs of 6.48–6.66. Significantly for our biogeophysical interpretation (section 5), it was concluded that the strong EM-31 anomaly most likely reflected a shallow aerobic perched water body that contains conductive materials as described above. The EM61 data (not presented) highlighted only discontinuous sections of pipework and reinforced concrete.

4.2. Contaminant Biogeochemistry Identified by the Intrusive Investigation

[11] The contaminant of concern, or risk driver, for permeable reactive barrier implementation are polycyclic aromatic hydrocarbons which are effectively degraded in a biological permeable reactive barrier (Tables 2 and 3; the full range of organic contaminants is not listed for clarity). For simplicity, solvent extractable matter is presented as representative of the sum of organic contaminants of concern (Figure 3a). It is reported as the aliquot of the Soxhlet extraction of the soil sample, from which further organic fractions (mineral oil, non volatile aromatics) have been identified by chromatographic separation. Ammoniacal nitrogen, sulphate and total cyanide contaminants, commonly associated with the purification processes at former manufactured gas plants, are presented in aid of the biogeophysical interpretation. Groundwater field measurements (Eh and pH) from multilevel piezometers in boreholes are presented in Figure 2. Only a small proportion of indigenous microorganisms are likely to be culturable in a laboratory environment (about 0.1–10%), and replication of in situ conditions is almost impossible with bias playing a significant role in the cultivation of mixed microbial populations. Consequently an indication of the variety and composition of microbial species across the site was achieved using molecular genetic techniques (i.e., cloning and 16S rDNA gene sequencing). Variation in the microbial community structures was observed following the comparison of soil DNA samples and Table 4 summarizes the results of the cloning of 16SrDNA and sequencing experiments from DNA samples obtained from soils directly. Only unique sequences from over 100 clones are shown and this indicates that the Gram negative proteobacteria were found with β-proteobacteria (especially from the genus *Azoarcus),* γ-proteobacteria (genus *Pseudomonas*), and δ-proteobacteria (genus *Geobacter*) being represented.

4.3. Contaminant Transport Modeling

[12] The modeled contaminant plume used a single source at depth from the area of the tar well. This was compared with groundwater monitoring from the intrusive phase of the site investigation. The spatial distribution of the groundwater data set indicates a source at depth (tar well) and various shallow sources originating from demolished structures at the west of site. Taking these shallow or surface sources from buildings on western site of the site into account

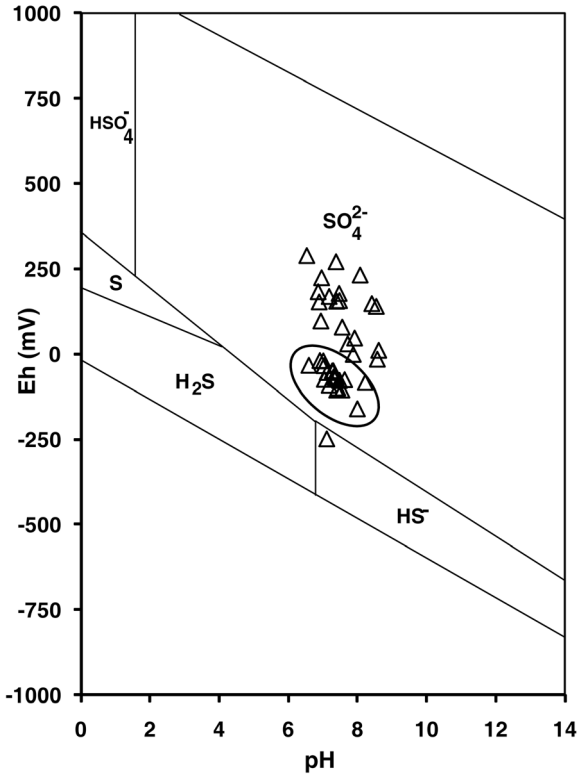

Figure 2. Eh versus pH scatterplot of groundwater samples from across the site. Samples from within the contaminant plume are enclosed in the ellipse.

there is still a good correlation between the modeled plume and measured solvent extractable matter in groundwater (Figure 3a). This provided assurance that the majority of groundwater contamination originates at depth (~5–7m below ground) from the tar well.

4.4. SP and IP Data

[13] An exceptionally strong dipolar self-potential anomaly (−455 mV to +380 mV), with a sharp negative-to-positive polarity switch over an East-West distance of less than 5 m, dominated the northeastern section of the site (Figure 4). Following correction of our self-potential data for groundwater flow-induced streaming potentials (as explained in *Revil et al.*, 2010), the residual self-potential map reflects electrochemically and biologically generated self-potential signals. The spatial extent of the strong dipolar self-potential anomaly agrees approximately with that of the conductive EM-31 anomaly (Figure 4), and therefore with that of the inferred shallow aerobic perched water body containing conductive materials. Significantly for our interpretation (section 5), the sharp transition zone marking the self-potential polarity switch coincides spatially with the eastern margin of the active microbial communities as inferred from total viable counts from soil samples (Figure 3b).

[14] Normalization of chargeabilities (section 3.4), by dividing our inverted induced polarization by the inverted resistivity data, allowed minimization of pore fluid electrical effects, including those of the inorganic conductive contaminants (ammonia and sulphate) in groundwater. We expect normalized chargeabilities to reflect buried metals, clays, bioprecipitation, mineralization or accumulations of microbes present in the pore space and attached to the solid matrix [*Reynolds*, 1997; *Sharma*, 1997; *Slater and Lesmes*, 2002; *Abdel Aal et al.*, 2004; *Ntarlagiannis et al.*, 2005; *Davis et al.*, 2006; *Ntarlagiannis and Ferguson*, 2009]. Significantly for our interpretation (section 5), the spatial extent of the most prominent normalized-chargeability anomaly agrees well with that of the positive portion of the strong dipolar self-potential anomaly (Figure 5). Several more minor normalized-chargeability anomalies are observed in the western and southern sectors, and are attributed to metallic objects left on site during the installation of the permeable reactive barrier or other demolition works. The resistivity anomaly (Figure 5d) occurs at depth below the maximum depth of trial pit sampling, preventing a chemical or microbial benchmark. The anomaly may be related to a mobile non aqueous phase liquid moving at the base of the contaminant plume [*Sentenac et al.*, 2009]. Further intrusive work is warranted to benchmark this anomaly.

5. Synthesis and Discussion

5.1. Conceptual Contaminant Biogeochemical Model

[15] The tar well at the southwestern part of site is the dominant source of organic contaminants in groundwater. Groundwater flowing in a northerly direction [*Doherty et al.*, 2003] is contaminated at depth (5–7m) by residual dense non aqueous phase liquids from the tar well. This plume is contained at depth by a thin clay aquiclude (0.5–2.5m) that covers the site. Ammonia was present as a liquid gasworks waste, known as *ammoniacal liquor* [*Hatheway*, 2002], and was usually disposed of in the tar well. Cyanide and sulphate compounds present as solid wastes were often reused as fill materials around the site [*Desrochers*, 2009]. In the concep-

t2.1 **Table 2.** Selected Groundwater Chemistry[a]

	Solvent Extractable Matter	Ammoniacal Nitrogen	Soluble Sulphate	Total Cyanide	Electrical Conductivity (μS/cm)
t2.2 Mean	9.5	120.5	806	5.6	1500
t2.3 Median	4.0	20.3	661	0.3	1240
t2.4 Mode	1.0	0.2[b]	2027.2	0.05[c]	
t2.5 Standard Deviation	15.7	177.4	687	14.4	790
t2.6 Minimum	1.0[d]	0.2[b]	52.4	0.05[c]	650
t2.7 Maximum	83.0	726.4	2814.1	85.1	3290
t2.8 Count	70	61	65	63	35

t2.9 [a]All results in ppm except electrical conductivity mS/cm. Non detects replaced by method detection limit.
t2.10 [b]Ammoniacal nitrogen 0.2ppm.
t2.11 [c]Total cyanide 0.05ppm.
t2.12 [d]Solvent extractable matter *1ppm.

t3.1 **Table 3.** Selected Soil Chemistry[a]

	Solvent Extractable Matter	Ammoniacal Nitrogen	Acid Soluble Sulphate (%)	Total Cyanide
t3.2 Mean	11641.5	69.5	0.5	508.5
t3.3 Median	1062	21.5	0.1	2.5[b]
t3.4 Mode	510	0.3[c]	0.01[d]	2.5[b]
t3.5 Standard deviation	36095	112.4	1.1	2025.9
t3.6 Minimum	13	0.3[c]	0.01[d]	2.5[b]
t3.7 Maximum	269080	605.7	7.1	13340.1
t3.8 Count	78	78	78	78

t3.9 [a]All results in ppm except acid soluble sulphate as %. Non Detects replaced by method detection limit.
t3.10 [b]Total cyanide 2.5ppm.
t3.11 [c]Ammoniacal nitrogen 0.3ppm.
t3.12 [d]Acid soluble sulphate 0.01%.

tual contaminant transport model of the site, ammonia occupies the same source area as the organic contaminants at the tar well. Cyanide and sulphate source areas are closer to the surface and are identified with structures or waste fill material. Elevated contaminant levels of ammonium of up to 726 ppm across the site, together with Eh pH measurements (Figure 2), suggest that the groundwater contaminants are in an anaerobic environment. Ammonium undergoes nitrification in an aerobic environment to form nitrate. *Broholm et al.* [1998] and *Torstensson et al.* [1998] noted that microbial oxidation of the ammonium in a former manufactured gas plant-type plume delineated the aerobic-anaerobic boundary within the contaminated groundwater. The elevated ammonium concentrations suggest that any available dissolved oxygen within the plume would be quickly depleted when nitrification of ammonium occurs. The molecular genetic techniques used to analyze soil bacteria at the site indicated that microorganisms of the proteobacteria were most common; especially those known to be associated with denitrification (Table 4). This indicates that the anaerobic utilization of nitrate was most likely. Ammonia dominates the contaminant biogeochemistry, preferentially sequestering dissolved oxygen. This in turn prevents aerobic biodegradation of organic compounds. Additional electron acceptors (sulphate reduction and methanogenesis) are also suppressed, as suggested by the groundwater Eh versus pH values (Figure 2) until the nitrogen electron acceptors (ammonia, nitrate and nitrite) are exhausted. Compound Specific Isotope Analysis work using Gas Chromatography - Mass Selective Detection - Isotope Ratio Mass Spectrometry from trial pit samples found that there was significant $\delta^{13}C$ variation depending on the matrix the contaminant was sampled from, and overall there was no conclusive evidence for widespread bioattenuation [*Hall*, 1999]. However, *Hall* [1999] noted $\delta^{13}C$ fractionation of residual aliphatic and phenolic compounds in groundwater. The majority of aerobic degradation of aromatic compounds is effectively stalled through oxygen depletion and possibly by the presence of ammonium, although there can still be a degree of anaerobic degradation of aliphatic and phenolic compounds. Total viable counts of aerobic microorganisms from soil samples [*Ferguson et al.*, 2003] reproduced here correlates well with contamination in groundwater (Figures 3a and 3b). Localized areas of low microbial viable counts at the plume can be attributed to surface structures,

t4.1 **Table 4.** Presumptive Phylogenetic Identification of Unique Eubacterial 16srDNAc Clones From Soil DNA Samples[a]

Phylogeny Group Assigned	Closest Homology (%) to Known 16srDNA Sequences	Physiological Type of Bacterium Known
t4.3 β-proteobacteria	-	-
t4.4 δ-Proteobacteria; Geobacteriaceae	92% *Geobacter* sp.	Metal-contaminated soil bacteria
t4.5 Firmicutes; Lactobacillaceae	98% *Lactosphera pasteurii*	Lactic acid bacteria
t4.6 β-proteobacteria	-	-
t4.7 β-proteobacteria; Rhodocyclus	90% *Azoarcus* sp.	Anaerobic bacteria
t4.8 β-proteobacteria; Comamonadaceae	91% *Rhodoferax* sp.	Denitrifying bacteria
t4.9 β-proteobacteria; Nitrosolobus	91% *Nitrosolobus multiformis*	Ammonium-oxidizing bacteria
t4.10 β-proteobacteria; Comamonadaceae	96% *Acidoferax* sp.	Denitrifying bacteria
t4.11 δ-Proteobacteria; Geobacteriaceae	91% *Geobacter arculus*	Humic acid-reducing bacterium
t4.12 β-proteobacteria; Rhodocyclus	95% unknown isolate H20	Denitrifying bacteria
t4.13 Unknown	-	-
t4.14 β-proteobacteria; Rhodocyclus	92% *Azoarcus evansii*	Denitrifying bacteria
t4.15 β-proteobacteria; Rhodocyclus	95% *Zoogloea* sp.	-
t4.16 γ-Proteobacteria; Pseudomonas	92% *Pseudomonas balearia*	Anaerobic thiosulfate degrading bacterium
t4.17 β-proteobacteria; Rhodocyclus	92% *Azoarcus* sp.	Denitrifying bacteria
t4.18 β-proteobacteria; Alcaligenaceae	93% *Alcaligenes* sp.	-
t4.19 β-proteobacteria; Comamonadaceae	95% *Rhodoferax antarticus*	-
t4.20 β-proteobacteria	-	Denitrifying bacteria
t4.21 β-proteobacteria	-	-
t4.22 β-proteobacteria; Burkholdera	96% *Herbaspirillium* sp.	Denitrifying bacteria
t4.23 γ-Proteobacteria; Pseudomonas	97% *Pseudomonas plecoglossicide*	Polycyclic aromatic hydrocarbon degrading bacterium
t4.24 Unknown	-	-
t4.25 β-proteobacteria	-	-

t4.26 [a]All clones were analyzed by restriction analysis using three restriction enzymes (*Alu*I, *Rsa*I, and *Hpa*II) to eliminate identical clones. Dash indicates
t4.27 where a close assignment could not be made.

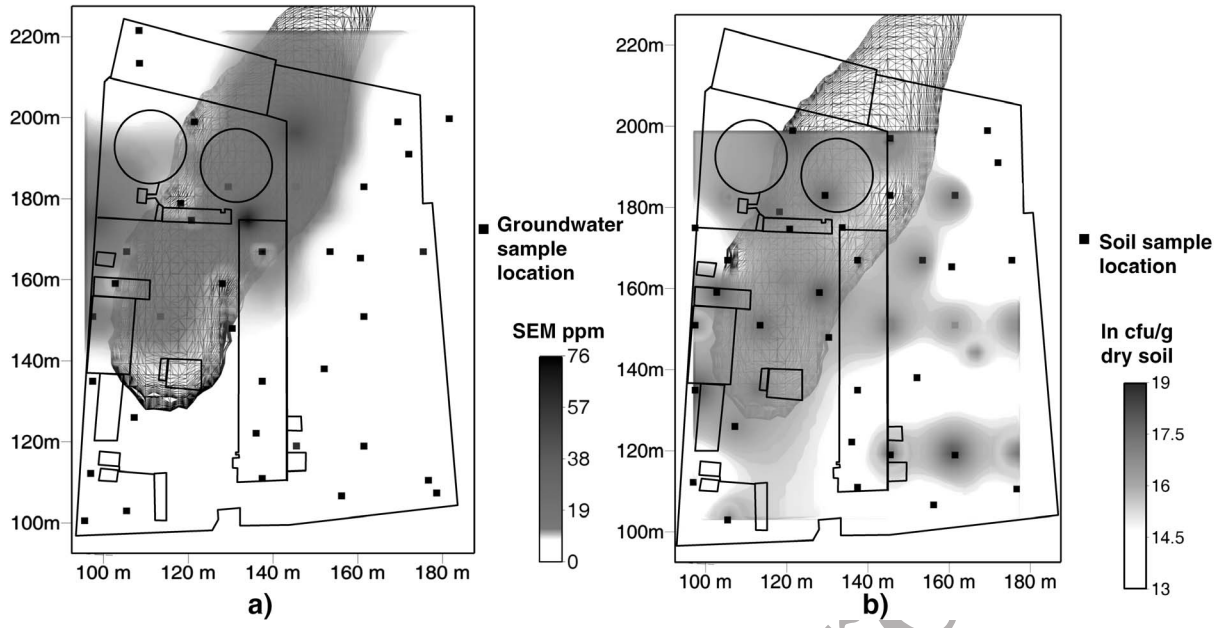

Figure 3. (a) Comparison of Solvent Extractable Matter (SEM) in groundwater as ppm (gray scale) with a modeled contaminant plume (black mesh) originating from the tar well at a depth of 5–7m. (b) Total viable microbial counts (ln cfu/g dry soil) as greyscale, note the microbial communities inferred from the total viable counts extend further to the east than the contaminant plume.

such as the purifiers and waste spoils that were localized sources of cyanide contamination and high pH. Relatively low microbial viable counts were also recorded in the pristine southeastern corner of the site (local grid 110N 170W) where no contaminating activities occurred, and where the SP reference electrode was located. A smaller separate set of viable counts (local grid 155N 160W) not based around the plume and tar well has been attributed to minor surface spills. This soil total viable count data is presented as inference of an active microbial community surrounding the organic contaminant plume [*Bakermans and Madsen*, 2000]. Recent work on similar sites suggests that microbial diversity is at a maximum at the plume edge, whereas only specific degraders can excel in the center of contaminant plumes where toxicity is greatest [*Ferguson et al.*, 2007]. The microbial community around the contaminant plume can be conceptualized as utilizing the contaminant plume as an energy source, mediating redox reactions and catalyzing contaminant degradation to provide a source of electrons (Figures 3a and 3b).

5.2. Microbial Fuel Cell as an Alternative to a Biogeobattery

[16] Field measurements revealed redox values ranging from +97 mV in the body of aerobic perched water to −161 mV in the anaerobic groundwater contaminant plume. The redox range between these bodies is narrow compared to the dipolar SP anomaly (>800 mV peak-to-peak). This narrow range of redox potential is not a large enough source mechanism to drive the observed electrical current flow as we would expect in a geochemically dominated, redox driven, geobattery model [*Arora et al.*, 2007] or biogeobattery model [*Revil et al.*, 2010], or to promote the precipitation of metal sulphides that contribute to IP responses reported by *Williams et al.* [2009] (Figure 2). The field SP response is an order of magnitude greater than the observed response from the corrosion of metallic objects as noted in laboratory experiments by *Castermant et al.* [2008], suggesting it is unlikely that the SP anomaly is due to corrosion of metallic debris in the

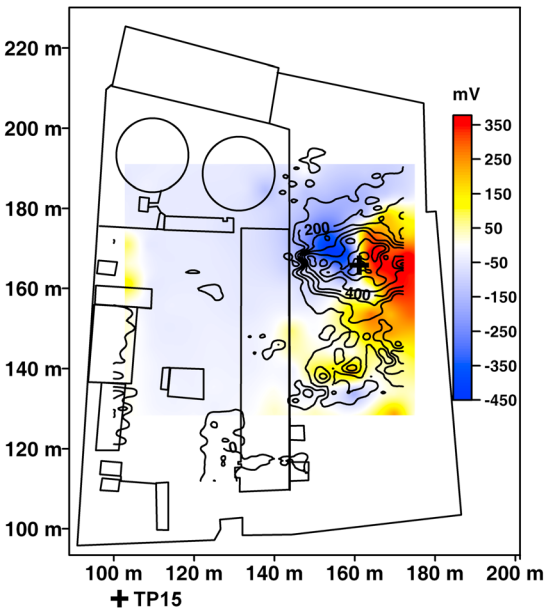

Figure 4. Dipolar self-potential anomaly (colors, mV) and contoured outlines of EM31 apparent conductivity (in mS/m). Note the sharp self-potential-polarity switch centered on Trial Pit 15 (labeled as a black cross).

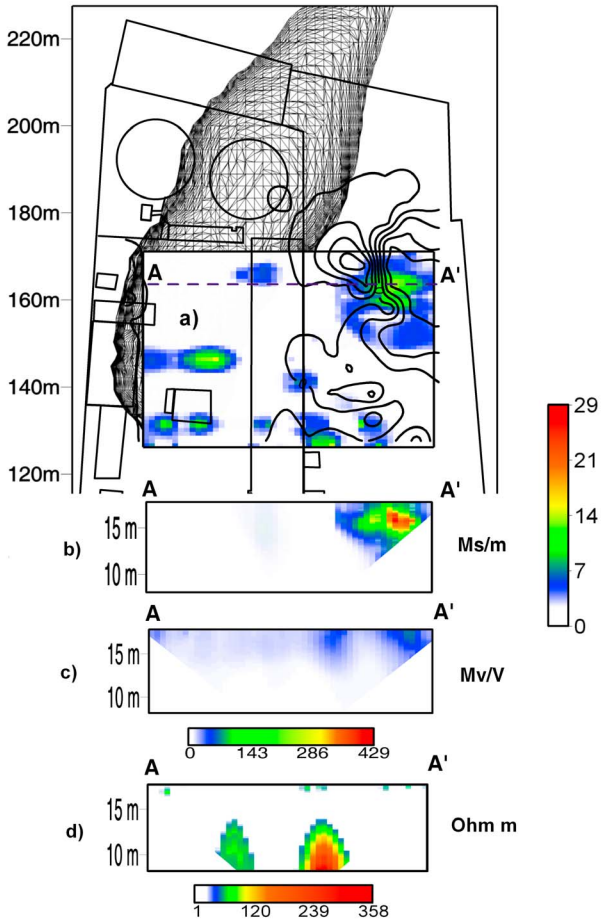

Figure 5. Plan of modeled contaminant plume (black mesh), contoured outlines of dipolar self-potential anomaly in mV (see Figure 4 for reference). (a) Chargeability normalized by resistivity (Ms/m) in color with 2D sections through line A-A′. (b) Chargeability normalized by resistivity (Ms/m). (c) Chargeability (Mv/V). (d) Resistivity (Ohm m).

perched water alone. In the absence of an alternative plausible explanation, we believe that the strong dipolar self-potential anomaly (Figure 4) reflects, instead, a microbial fuel cell [*He and Angenent*, 2006], which is theoretically well-founded [*Revil et al.*, 2010]. Microbial fuel cells generate electrical current by utilizing microbes to catalyze organic material producing electrons [*Du et al.*, 2007]; in this case the microbes catalyze the contaminant plume. As explained below, this cell is inferred to be characterized by a biological anode associated with the active microbial soil communities around the contaminant plume (as reflected by molecular genetic techniques; Table 4 and total viable counts; Figure 3b), an abiotic cathode associated with the metallic infill congregated within the aerobic body of perched water (as reflected by the pronounced normalized-chargeability anomaly; Figure 5), and a locally punctured clay aquiclude around trial pit 15 that facilitates transfer of charge and acts as an electronic conductor interconnecting the biological anode and the abiotic cathode. We use the term microbial fuel cell rather than biogeobattery due to the fact that our conceptual model proposes a biological anode and abiotic cathode rather than a series of biologically mediated electron acceptors acting as the anode and cathode.

5.3. Biological Anode

[17] The anaerobic conditions in the organic contaminant plume can readily provide negatively charged conditions (Figure 2). The active anaerobic microbial soil communities could furnish an efficient mechanism allowing electron flow in the areas adjacent to the contaminant plume (Figure 3b). There is still much debate over mechanisms that allow electron transfer from microbial cells [*Lovley*, 2008a, 2008b]. The mechanisms can be generally split in two categories, transfer of electrons using nanowires or pili [*Reguera et al.*, 2005; *Gorby et al.*, 2006; *Ntarlagiannis et al.*, 2007; *Gorby et al.*, 2008], or transfer of electrons using soluble recalcitrant organic electron shuttles such as flavin [*Velasquez-Orta et al.*, 2009] or naturally occurring humic materials [*Newman and Kolter*, 2000]. Site specific microbial data (cloning and 16S rDNA gene sequencing) suggest humic reducing microbes are established in soil samples (Table 4). In all of the above, the transfer of scale from mechanisms occurring at the cell to measurements in the field is important. The models proposed by *Revil et al.* [2010] allow the aggregation of microscale electron transfer (either between cells or between cells and precipitates/aquifer media) to create macroscopic dipoles. Specifically, this would allow the microbial soil communities on the eastern side of the contaminant plume (Figure 3b) to act as an anode. This area of the microbial soil communities are marked by negative SP values up to the sharp polarity switch at the plume's eastern margin. The site-specific microbial data (cloning and 16S rDNA gene sequencing) reveal that electrons cannot only come from microbial utilization of contaminant organic matter [*Atekwana et al.*, 2005; *Du et al.*, 2007; *Revil et al.*, 2010], but also from mechanisms that involve ammonia-oxidizing chemoautotrophs such as β-Proteobacetria (*Nitrosolobus spp*) [*Head et al.* 1993]

$$NH^{4+} + O_2 \rightarrow NO_2^- + 4H^+ + 2e- \quad (1)$$

Many nitrifying or nitrate reducing bacteria were established as common in soil at the site (Table 4) and this suggests nitrate production and nitrification is also very important:

$$2NO^{2-} + H_20 \rightarrow 2NO^{3-} + 2H^+ + 2e- \quad (2)$$

Equations (1) and (2) are consistent with the strong possibility of an effective biologically dominated anode that couples the contaminant plume with the surrounding microbial architecture, including ammonia oxidizers, nitrate reducers and organic contaminant degraders acting as the *electrode reducers* [*Lovley*, 2008a].

5.4. Abiotic Cathode

[18] In the search for an abiotic cathode we recall that the spatial extent of most the prominent normalized-chargeability anomaly agrees well with the positive portion of the strong dipolar self-potential anomaly (Figure 5). In the absence of an alternative plausible explanation, we postulate that the mechanism generating this anomaly could also act as the abiotic cathode of our microbial fuel cell. Indeed, the normalized-chargeability anomaly probably delineates

the ash, clinker and iron compounds that were discovered and back-filled during trial-pitting. These compounds are congregated within the shallow body of perched groundwater delineated by our EM-31 data (compare Figures 1 and 5). We therefore believe that geochemical reactions within these oxygen-rich waters are oxidizing the waste-iron compounds, effectively acting as the abiotic cathode of our microbial fuel cell. We do note that microbiological analysis has also identified denitrifying bacteria which could potentially compete with the abiotic cathode for electrons.

5.5. Interconnecting Electronic Conductor

[19] Trial-pitting (TPs 15 and 32) confirmed that a shallow body of perched aerobic water and backfilled conductive waste overlying a layer of clay, as delineated by the EM-31 data (Figures 1 and 4). We interpret this as the abiotic cathode delineated by the normalized-chargeability anomaly that is also present (Figure 5). The clay layer separating the perched water and contaminant plume effectively divides these bodies into an abiotic cathode chamber (perched water) and a biological anode chamber (contaminant plume). The clay layer was thinned and probably punctured during the excavation of TP 15 which sits in the center of the SP dipole (Figures 4 and 5), connecting the oxidizing body of perched waters above it with the reducing environment beneath it. A microbial fuel cell requires a cation-exchange membrane that allows cations or protons to diffuse and thus allow the anode to operate efficiently [*Rozendal et al.*, 2006]. This punctured clay layer, backfilled with conductive waste, may act as an exchange membrane or electronic conductor connecting the contaminant plume, the biological anode of our microbial fuel cell, to the normalized-chargeability anomaly representing the abiotic cathode within the shallow body of perched water (Figures 1 and 5). This would support a situation where the contaminant plume and electrode reducers provide electrons that reduce the waste-iron compounds to Fe (II):

$$Fe^{3+} + e^- \rightarrow Fe^{2+} \quad (3)$$

The aerobic water above could oxidize the reduced iron to Fe (III):

$$4Fe^{2+} + O_2 + 4H^+ \rightarrow 4Fe^{3+} + 2H_2O \quad (4)$$

The waste-iron compounds backfilled in TPs 15, 32 and 33 (Figure 1) would, thus, act as electrode mediators between oxygen, derived from the aerobic perched waters (dissolved oxygen measured in TP15 ranged from 0.11 to 1.01ppm and redox potential was 67–97mV, section 4.1), and the abiotic cathode, where oxygen is the terminal electron acceptor [*Park and Zeikus*, 2003; *He and Angenent*, 2006]:

$$14e^- + 3.5O_2 + 14H^+ \rightarrow 7H_2O. \quad (5)$$

5.6. Implications for the Sustainable Remediation of Contaminated Land

[20] The use of multiple geophysics methods (electromagnetic, self-potential, induced polarization and resistivity) alongside chemical and microbiological analysis has been invaluable in developing and quantifying site conceptual models and the management of a site remediation strategy. The use of electrical geophysical methods as remediation monitoring tools has provided additional insight to a complex biogeochemical environment. The large self-potential response is probably generated by contaminant biodegradation providing a source of electrons to the fuel cell. This has implications for our ability to actively monitor biodegradation in contaminant plumes. Demonstration of ongoing biodegradation is a requirement for remediation methods such as monitored natural attenuation. This is often the most technically difficult, expensive and intrusive aspect of the monitoring process. The electrical geophysical methods show promise as inexpensive, non intrusive, real time methods. These are the qualities of 'sustainable remediation' tools [*Spira*, 2006; *U.S. Sustainable Remediation Forum*, 2009] that are required if contaminated land issues are to be managed efficiently in the future. Further work is still required to develop field scale abiotic self-potential cathodes to complete the flow of electrons from biodegrading plumes that act as bio-anodes or to enhance biodegradation [*Zhang et al.*, 2010]. The use of electrical geophysical methods could have further applications in more controlled engineered environments where biodegradation or microbial activity occurs, for example, municipal wastewater systems, landfill and leachate treatment, anaerobic digestion of wastes using mechanical - biological treatment and monitoring of industrial biofouling.

6. Conclusions

[21] The revised conceptual model of the site considers a contaminant plume from the tar well. The plume consists predominately of organic contaminants and inorganic ammonia disposed of below the water table. Total viable counts from soil samples, as well as cloning and 16S rDNA sequencing, provides assurance that the plume has a diverse microbial community around it. An exceptionally strong, dipolar self-potential anomaly (>800 mV peak-to-peak after correction for streaming potential) is inferred to be generated by a microbial fuel cell operating in the eastern sector of the site. The contaminant biogeochemistry is dominated by ammonia, oxidation to nitrate and subsequent reduction along with some biodegradation of aliphatic and phenolic compounds. This reducing environment and associated biodegradation around the contaminant plume is proposed as an anode of the microbial fuel cell producing electrons. A congregation of waste-iron compounds, back-filled after trial-pitting and situated within a shallow body of aerobic perched water, is inferred to act as the cell's abiotic cathode. The perched-water body and the waste-iron compounds within it were respectively delineated as strong EM-31 and normalized-chargeability anomalies. This body of aerobic perched water, and thus the waste-iron compounds, overlie a clay layer which has been thinned and probably punctured during the intrusive site investigation. This thinned and punctured clay could now act as a permeable membrane allowing ion and electron transport between the electron-providing anode and the oxidizing cathode, thus acting as an interconnecting electronic conductor of the microbial fuel cell. The transport of electrons from the anode is probably provided by an aggregation of microscale cell to cell, or cell to aquifer electron transfer to the punctured aquiclude; where geochemical reduction and oxidation of iron compounds takes place. From our field data we cannot

attribute a specific mechanism of electron transport from microbial communities; possibilities are electron shuttling from naturally occurring humic compounds, extracellular transfer across pili or a combination of the two. Further work is warranted to define the modes of electron transport and/or electronic conductors. In this case, geophysics provided assurance that microbially dominated conditions around the plume were present and active. The spatial distribution of the geophysical measurements around the contaminant plume and perched water suggests that microbial fuel cells do function without assistance in anthropogenic environments outside of the laboratory. This has future applications in terms of design, engineering and monitoring of biological systems as proposed by *Curtis et al.* [2003].

[22] **Acknowledgments.** This research was supported by EPSRC grant GR/M89768/01, the Department for the Environment Northern Ireland, the Questor Centre, and Keller Ground Engineering Ltd. A. Brown and A. de Jong collected the EM data. David Leemon and John Patterson collected the SP, IP and resistivity data, and Valerie Irvine supported the microbiological analyses. We would also like to thank the constructive and helpful comments of the reviewers.

References

Abdel Aal, G. Z., E. A. Atekwana, L. D. Slater, and E. A. Atekwana (2004), Effects of microbial processes on electrolytic and interfacial electrical properties of unconsolidated sediments, *Geophys. Res. Lett.*, *31*, L12505, doi:10.1029/2004GL020030.

Arora, T., N. Linde, A. Revil, and J. Castermant (2007), Non-intrusive characterization of the redox potential of landfill leachate plumes from self-potential data, *J. Contam. Hydrol.*, *92*, 274–292, doi:10.1016/j.jconhyd.2007.01.018.

Atekwana, E. A., E. Atekwana, F. D. Legall, and R. V. Krishnamurthy (2005), Biodegradation and mineral weathering controls on bulk electrical conductivity in a shallow hydrocarbon contaminated aquifer, *J. Contam. Hydrol.*, *80*, 149–167, doi:10.1016/j.jconhyd.2005.06.009.

Bakermans, C., and E. L. Madsen (2000), Use of substrate responsive-direct viable counts to visualize naphthalene degrading bacteria in a coal tar-contaminated groundwater microbial community, *J. Microbiol. Methods*, *43*(2), 81–90, doi:10.1016/S0167-7012(00)00210-4.

Bigalke, J., and E. W. Grabner (1997), The Geobattery model: A contribution to large scale electrochemistry, *Electrochim. Acta*, *42*(23–24), 3443–3452, doi:10.1016/S0013-4686(97)00053-4.

Broholm, M. M., I. Jones, D. Torstensson, and E. Arvin (1998), Groundwater contamination from a coal carbonisation plant, in *Contaminated Land and Groundwater: Future Directions*, edited by D. N. Lerner and N. Walton, pp. XX–XX, Geol. Soc., London.

Bullen, R. A., T. C. Arnot, J. B. Lakeman, and F. C. Walsh (2006), Biofuel cells and their development, *Biosens. Bioelectron.*, *21*(11), 2015–2045, doi:10.1016/j.bios.2006.01.030.

Castermant, J., C. A. Mendonça, A. Revil, F. Trolard, G. Bourrié, and N. Linde (2008), Redox potential distribution inferred from self-potential measurements associated with the corrosion of a burden metallic body, *Geophys. Prospect.*, *56*(2), 269–282, doi:10.1111/j.1365-2478.2007.00675.x.

Curtis, T. P., I. M. Head, and D. W. Graham (2003), Theoretical ecology for engineering biology, *Environ. Sci. Technol.*, *37*(3), 64A–70A, doi:10.1021/es0323493.

Davis, C. A., E. A. Atekwana, E. Atekwana, L. D. Slater, S. Rossbach, and M. R. Mormille (2006), Microbial growth and biofilm formation in geologic media is detected with complex conductivity measurements, *Geophys. Res. Lett.*, *33*, L18403, doi:10.1029/2006GL027312.

Desrochers, P. (2009), Does the invisible hand have a green thumb? Incentives, linkages, and the creation of wealth out of industrial waste in Victorian England, *Geogr. J.*, *175*(1), 3–16, doi:10.1111/j.1475-4959.2008.00315.x.

Doherty, R., U. S. Ofterdinger, Y. Yang, K. Dickson, and R. M. Kalin (2003), Observed and modelled hydraulic aquifer response to slurry wall installation at the former Gasworks Site, in *Advanced Groundwater Remediation: Active and Passive Technologies*, edited by F. G. Simon, T. Meggyes, and C. M. McDonald, pp. XX–XX, Thomas Telford, Portadown, U. K.

Du, Z., H. Li, and T. Gu (2007), A state of the art review on microbial fuel cells: A promising technology for wastewater treatment and bioenergy, *Biotechnol. Adv.*, *25*(5), 464–482, doi:10.1016/j.biotechadv.2007.05.004.

Ferguson, A. S., R. Doherty, M. J. Larkin, R. M. Kalin, V. Irvine, and U. S. Ofterdinger (2003), Toxicity assessment of a former manufactured gas plant, *Bull. Environ. Contam. Toxicol.*, *71*(1), 21–30, doi:10.1007/s00128-003-0125-y.

Ferguson, A. S., et al. (2007), Microbial analysis of soil and groundwater from a gasworks site and comparison with a sequenced biological reactive barrier remediation process, *J. Appl. Microbiol.*, *102*(5), 1227–1238, doi:10.1111/j.1365-2672.2007.03398.x.

Fournier, C. (1989), Spontaneous potentials and resistivity surveys applied to hydrogeology in a volcanic area: Case history of the Chaine des Puys (Puy-de-Dome, France), *Geophys. Prospect.*, *37*, 647–668, doi:10.1111/j.1365-2478.1989.tb02228.x.

Gibert, O., A. S. Ferguson, R. M. Kalin, R. Doherty, K. W. Dickson, K. L. McGeough, J. Robinson, and R. Thomas (2007), Performance of a sequential reactive barrier for bioremediation of coal tar contaminated groundwater, *Environ. Sci. Technol.*, *41*(19), 6795–6801, doi:10.1021/es071527f.

Gorby, Y. A., et al. (2006), Electrically conductive bacterial nanowires produced by Shewanella oneidensis strain MR-1 and other microorganisms, *Proc. Natl. Acad. Sci. U. S. A.*, *103*(30), 11,358–11,363, doi:10.1073/pnas.0604517103.

Gorby, Y., J. Mclean, A. Korenevsky, K. Rosso, M. Y. El-Naggar, and T. J. Beveridge (2008), Redox-reactive membrane vesicles produced by *Shewanella*, *Geobiology*, *6*(3), 232–241, doi:10.1111/j.1472-4669.2008.00158.x.

Hall, J. (1999), Stable isotope methods for monitoring bioremediation of contaminated land Ph.D. thesis, Queen's Univ. of Belfast, Belfast.

Hatheway, A. W. (2002), Geoenvironmental protocol for site and waste characterization of former manufactured gas plants: Worldwide remediation challenge in semi-volatile organic wastes, *Eng. Geol.*, *64*(4), 317–338, doi:10.1016/S0013-7952(01)00097-7.

He, Z., and L. T. Angenent (2006), Application of bacterial biocathodes in microbial fuel cells, *Electroanalysis*, *18*(19–20), 2009–2015, doi:10.1002/elan.200603628.

Head, I. M., W. D. Hiorns, M. T. Embley, A. J. McCarthy, and J. R. Saunders (1993), The phylogeny of autotrophic ammonia-oxidizing bacteria as determined by analysis of 16S ribosomal RNA gene sequences, *J. Gen. Microbiol.*, *139*, 1147–1153.

Kalin, R. M. (2004), Engineered passive bioreactive barriers: Risk-managing the legacy of industrial soil and groundwater pollution, *Curr. Opin. Microbiol.*, *7*, 227–238, doi:10.1016/j.mib.2004.04.014.

Kulessa, B., B. Hubbard, and G. H. Brown (2003), Cross-coupled flow modeling of coincident streaming and electrochemical potentials and application to subglacial self-potential data, *J. Geophys. Res.*, *108*(B8), 2381, doi:10.1029/2001JB001167.

LaBrecque, D., and W. Daily (2008), Assessment of measurement errors for galvanic-resistivity electrodes of different composition, *Geophysics*, *73*, F55–F64, doi:10.1190/1.2823457.

Leu, J. Y., C. P. McGovern-Traa, A. J. R. Poter, W. J. Harris, and W. A. Hamilton (1998), Identification and phylogenetic analysis of thermophilic sulphate-reducing bacteria in oil fuel samples by 16S rDNA gene cloning and sequencing, *Anaerobe*, *4*, 165–174, doi:10.1006/anae.1998.0156.

Linde, N., A. Revil, A. Bolève, C. Dagès, J. Castermant, B. Suski, and M. Voltz (2007), Estimation of the water table throughout a catchment using self-potential and piezometric data in a Bayesian framework, *J. Hydrol.*, *334*(1–2), 88–98, doi:10.1016/j.jhydrol.2006.09.027.

Loke, M. H., and R. D. Barker (1996), Rapid least-squares inversion of apparent resistivity pseudosections by a quasi-Newton method, *Geophys. Prospect.*, *44*(1), 131–152, doi:10.1111/j.1365-2478.1996.tb00142.x.

Lovley, D. R. (2008a), The microbe electric: Conversion of organic matter to electricity, *Curr. Opin. Biotechnol.*, *19*(6), 564–571, doi:10.1016/j.copbio.2008.10.005.

Lovley, D. R. (2008b), Extracellular electron transfer: Wires, capacitors, iron lungs, and more, *Geobiology*, *6*(3), 225–231, doi:10.1111/j.1472-4669.2008.00148.x.

Maineult, A., Y. Bernabé, and P. Ackerer (2006), Detection of advected, reacting redox fronts from self-potential measurements, *J. Contam. Hydrol.*, *86*(1–2), 32–52, doi:10.1016/j.jconhyd.2006.02.007.

Minsley, B. J., J. Sogade, and F. D. Morgan (2007), Three-dimensional self-potential inversion for subsurface DNAPL contaminant detection at the Savannah River Site, South Carolina, *Water Resour. Res.*, *43*, W04429, doi:10.1029/2005WR003996.

Naudet, V., and A. Revil (2005), A sandbox experiment to investigate bacteria-mediated redox processes on self-potential signals, *Geophys. Res. Lett.*, *32*, L11405, doi:10.1029/2005GL022735.

Naudet, V., A. Revil, E. Rizzo, J. Y. Bottero, and P. Bagassat (2004), Groundwater redox conditions and conductivity in a contaminant plume from geoelectrical investigations, *Hydrol. Earth Syst. Sci.*, *8*(1), 8–22, doi:10.5194/hess-8-8-2004.

Newman, D. K., and R. Kolter (2000), A role for excreted quinones in extracellular electron transfer, *Nature*, *405*(6782), 94–97, doi:10.1038/35011098.

Ntarlagiannis, D., and A. Ferguson (2009), SIP response of artificial biofilms, *Geophysics*, *74*(1), A1–A5, doi:10.1190/1.3031514.

Ntarlagiannis, D., N. Yee, and L. D. Slater (2005), On the low-frequency electrical polarization of bacterial cells in sands, *Geophys. Res. Lett.*, *32*, L24402, doi:10.1029/2005GL024751.

Ntarlagiannis, D., E. A. Atekwana, E. A. Hill, and Y. Gorby (2007), Microbial nanowires: Is the subsurface "hardwired"?, *Geophys. Res. Lett.*, *34*, L17305, doi:10.1029/2007GL030426.

Park, D. H., and J. G. Zeikus (2003), Improved fuel cell and electrode designs for producing electricity from microbial degradation, *Biotechnol. Bioeng.*, *81*(3), 348–355, doi:10.1002/bit.10501.

Patella, D. (1997), Introduction to ground surface self-potential tomography, *Geophys. Prospect.*, *45*(4), 653–681, doi:10.1046/j.1365-2478.1997.430277.x.

Personna, Y. R., D. Ntarlagiannis, L. Slater, N. Yee, M. O'Brien, and S. Hubbard (2008), Spectral induced polarization and electrodic potential monitoring of microbially-mediated iron sulfide transformations, *J. Geophys. Res.*, *113*, G02020, doi:10.1029/2007JG000614.

Petiau, G. (2000), Second generation of lead-lead chloride electrodes for geophysical applications, *Pure Appl. Geophys.*, *157*, 357–382, doi:10.1007/s000240050004.

Reguera, G., K. D. McCarthy, T. Mehta, J. S. Nicoll, M. T. Tuominen, and D. R. Lovley (2005), Extracellular electron transfer via microbial nanowires, *Nature*, *435*(7045), 1098–1101, doi:10.1038/nature03661.

Revil, A., V. Naudet, J. Nouzaret, and M. Pessel (2003), Principles of electrography applied to self-potential electrokinetic sources and hydrogeological applications, *Water Resour. Res.*, *39*(5), 1114, doi:10.1029/2001WR000916.

Revil, A., F. Trolard, G. Bourrié, J. Castermant, A. Jardani, and C. A. Mendonça (2009), Ionic contribution to the self-potential signals associated with a redox front, *J. Contam. Hydrol.*, *109*(1–4), 27–39, doi:10.1016/j.jconhyd.2009.07.008.

Revil, A., C. A. Mendonça, E. A. Atekwana, B. Kulessa, S. Hubbard, and K. Bohlen (2010), Understanding biogeobatteries: Where geophysics meets microbiology, *J. Geophys. Res.*, *115*, G00G02, doi:10.1029/2009JG001065.

Reynolds, J. M. (1997), *An Introduction to Applied and Environmental Geophysics*, John Wiley, Chichester, U. K.

Rozendal, R. A., H. V. M. Hamelers, and C. J. N. Buisman (2006), Effects of membrane cation transport on pH and microbial fuel cell performance, *Environ. Sci. Technol.*, *40*(17), 5206–5211, doi:10.1021/es060387r.

Sambrook, J., T. Maniatis, and E. F. Fritsch (1989), *Molecular Cloning: A Laboratory Manual*, 2nd ed., Cold Spring Harbor Lab., New York.

Sandberg, S. K., L. D. Slater, and R. Versteeg (2002), An integrated geophysical investigation of the hydrogeology of an anisotropic unconfined aquifer, *J. Hydrol.*, *267*(3–4), 227–243, doi:10.1016/S0022-1694(02)00153-1.

Sato, M., and H. M. Mooney (1960), The electrochemical mechanism of sulfide self-potentials, *Geophysics*, *25*(1), 226–249, doi:10.1190/1.1438689.

Sentenac, P., A. Montinaro, and B. Kulessa (2009) Diesel transport monitoring in simulated unconfined aquifers using miniature resistivity arrays, *Environ. Earth Sci.*, doi:10.1007/s12665-009-0325-9, in press.

Sharma, P. (1997), *Environmental and Engineering Geophysics*, Cambridge Univ. Press, Cambridge, U. K.

Slater, L., and A. Binley (2006), Synthetic and field-based electrical imaging of a zerovalent iron barrier: Implications for monitoring long-term barrier performance, *Geophysics*, *71*(5), B129–B137, doi:10.1190/1.2235931.

Slater, L. D., and D. Lesmes (2002), IP interpretation in environmental investigations, *Geophysics*, *67*, 77–88, doi:10.1190/1.1451353.

Slater, L., D. Ntarlagiannis, Y. R. Personna, and S. Hubbard (2007), Pore-scale spectral induced polarization signatures associated with FeS biomineral transformations, *Geophys. Res. Lett.*, *34*, L21404, doi:10.1029/2007GL031840.

Spira, Y., J. Henstock, P. Nathanail, D. Müller, and D. Edwards (2006), A European approach to increase innovative soil and groundwater remediation technology applications, *Rem. J.*, *16*(4), 81–96, doi:10.1002/rem.20103.

Torstensson, D., S. F. Thornton, M. M. Broholm, and D. N. Lerner (1998), Hydrochemistry of pollutant attenuation in groundwater contaminated by coal tar wastes, in *Contaminated Land and Groundwater: Future Directions*, edited by D. N. Lerner and N. Walton, pp. XX–XX, Geol. Soc., London.

U.S. Sustainable Remediation Forum (2009), Sustainable remediation white paper—Integrating sustainable principles, practices, and metrics into remediation projects, *Rem. J.*, *19*(3), 5–114, doi:10.1002/rem.20210.

Velasquez-Orta, S., I. Head, T. Curtis, K. Scott, J. Lloyd, and H. von Canstein (2009), The effect of flavin electron shuttles in microbial fuel cells current production, *Appl. Microbiol. Biotechnol.*, *85*, 1373–1381, doi:10.1007/s00253-009-2172-8.

Williams, K. H., A. Kemna, M. J. Wilkins, J. Druhan, E. Arntzen, A. L. N'Guessan, P. E. Long, S. S. Hubbard, and J. F. Banfield (2009), Geophysical monitoring of coupled microbial and geochemical processes during stimulated subsurface bioremediation, *Environ. Sci. Technol.*, *43*(17), 6717–6723, doi:10.1021/es900855j.

Zhang, T., S. M. Gannon, K. P. Nevin, A. E. Franks, and D. R. Lovley (2010), Stimulating the anaerobic degradation of aromatic hydrocarbons in contaminated sediments by providing an electrode as the electron acceptor, *Environ. Microbiol.*, *12*(4), 1011–1020, doi:10.1111/j.1462-2920.2009.02145.x.

R. Doherty, Environmental Engineering Research Centre, School of Planning Architecture and Civil Engineering, Queen's University of Belfast, Belfast BT9 5AG, UK. (r.doherty@qub.ac.uk)

A. S. Ferguson, Department of Civil Engineering and Engineering Mechanics, Columbia University, New York, NY 10027, USA. (af2460@columbia.edu)

R. M. Kalin, David Livingstone Centre for Sustainability, Department of Civil Engineering, Strathclyde University, Glasgow G4 ONG, UK. (robert.kalin@strath.ac.uk)

L. A. Kulakov and M. J. Larkin, QUESTOR Centre, Queen's University of Belfast, Belfast BT9 7BL, UK. (l.kulakov@qub.ac.uk; m.larkin@qub.ac.uk)

B. Kulessa, School of the Environment and Society, Swansea University, Swansea SA2 8PP, UK. (b.kulessa@swansea.ac.uk)